Analytical Methods

Accepted Manuscript

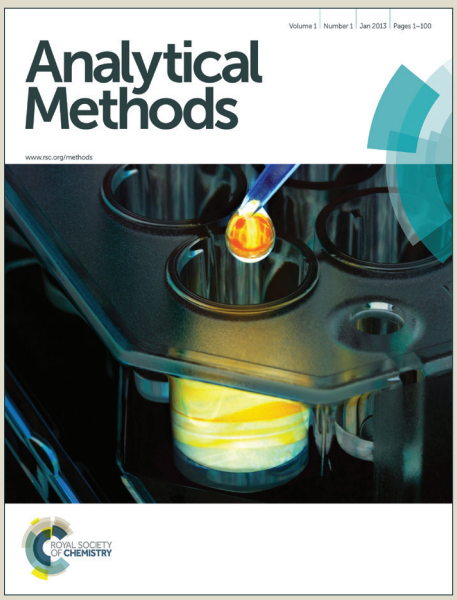

This is an *Accepted Manuscript*, which has been through the Royal Society of Chemistry peer review process and has been accepted for publication.

Accepted Manuscripts are published online shortly after acceptance, before technical editing, formatting and proof reading. Using this free service, authors can make their results available to the community, in citable form, before we publish the edited article. We will replace this *Accepted Manuscript* with the edited and formatted *Advance Article* as soon as it is available.

You can find more information about *Accepted Manuscripts* in the Information for Authors.

ROYAL SOCIETY OF CHEMISTRY

www.rsc.org/methods

Quantitative investigation on the dynamic interaction of human serum albumin with procaine using multi-way calibration method coupled with three-dimensional fluorescence spectroscopy

Li-Xia Xie, Hai-Long Wu*, Chao Kang, Shou-Xia Xiang, Xiao-Li Yin, Hui-Wen Gu, Qi Zuo, Ru-Qin Yu

State Key Laboratory of Chemo/Biosensing and Chemometrics, College of Chemistry and Chemical Engineering, Human University, Changsha 410082, China

* Corresponding author. Tel.: +86 731 88821818; Fax: +86 731 88821818.

E-mail address: hlwu@hnu.edu.cn (Hai-Long Wu).

Table of contents entry: The free human serum albumin in dynamic interaction system is quantified using multi-way calibration method coupled with three-dimensional fluorescence spectroscopy.

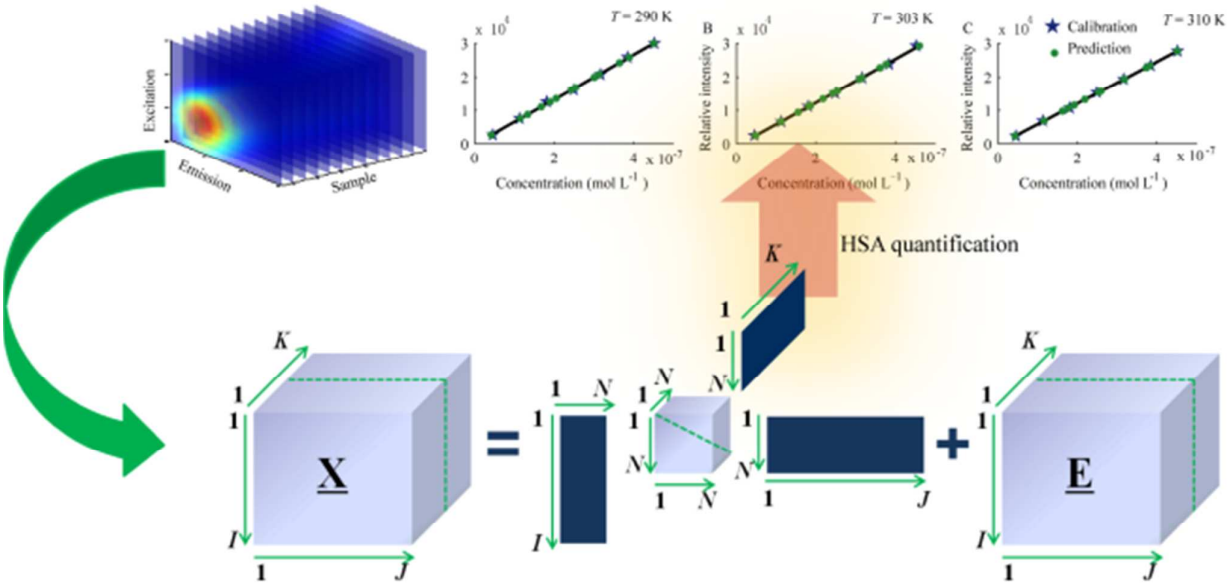

Abstract

In fluorospectrophotometric studies on protein-drug interactions, the fluorescence intensity of proteins is often vulnerable to interference from ligands or new produced complexes which exhibit significant fluorescence at the chosen excitation or emission wavelengths. Alternatively, this paper suggested an effective and sensitive method for quantitative determination of the free human serum albumin (HSA) in a dynamic interaction system with procaine (PRO) and further investigation on their interaction mechanism using multi-way calibration method coupled with three-dimensional fluorescence spectroscopy. Second-order calibration method realized the quantitative determination of the free HSA in a dynamic system with overlapping spectra even in the presence of an uncalibrated interferent. The quantitative results were used to further calculate the binding parameters, including binding constant, binding site number, thermodynamic parameters and nature of the binding forces. Furthermore, the four-way excitation-emission-temperature-sample data were analyzed to investigate the effect of temperature on the interaction system studied.

Keywords: Human serum albumin; Procaine; Dynamic interaction system; Multi-way calibration method; Three-dimensional fluorescence spectroscopy.

1. Introduction

Human serum albumin (HSA), as the major soluble protein constituent of the circulatory system, plays a dominant role in transport and disposition of numerous endogenous and exogenous substances in blood [1]. The affinity of biologically active substances toward HSA can be mainly responsible for the events involved in absorption, distribution, metabolism and excretion [2, 3]. Typically, a weak binding shows such a short lifetime to insufficiently provide its therapeutic effect, whereas a strong binding decreases the free fraction of drugs with undesirable side effects because of its too slow metabolism and excretion [4]. Consequently, investigations on binding mechanism of drugs to HSA are of fundamental importance, which can potentially provide an insight into pharmacokinetics and pharmacodynamics of drugs and design of dosage form.

Structurally, HSA contains a single intrinsic tryptophan residue, whose fluorescence is susceptible to the nearby drugs [5, 6]. Therefore, spectrofluorimetry with high sensitivity and low detection limit has been proposed as a reliable method to investigate drug-albumin interaction systems, where information about structural features of HSA, small drug molecules and drug-protein complexes can be revealed by the measurement of intrinsic fluorescence before and after addition of drugs [7, 8]. A literature search shows that fluorescence quenching has been favored by researchers to characterize the protein binding of drugs [9-13]. However, in fluorospectrophotometric studies on protein-drug interactions, the fluorescence intensity of proteins is often vulnerable to interference from ligands or new produced complexes which exhibit significant fluorescence at the chosen excitation or emission wavelengths. Therefore, a rather large number of studies involving the fluorescence methodology appear to assume a non-fluorescent complex existing in drug-protein interaction and calculate relevant binding constants by the ratio of HSA fluorescence intensity before

and after additional drugs, which frequently lead to an erroneous result.

With a variety of second- and higher-order experimental data being produced by modern instruments, multi-way data analysis, which is one of the most active areas in chemometrics, has been flourishing in the application of complex matrixes over the last few decades. A series research reveal that multi-way data analysis has been widely used in static systems, including those found in biological [14], environmental [15] and food samples [16, 17], etc., as there are increasing applications in dynamic systems including hydrolysis kinetics [18], enzymatic reaction kinetics [19, 20], etc. Some literatures have been contributed to investigation on drug-biomacromolecule interactions using chemometric method [21-25]. Zhou et al. studied the interaction of pirarubicin with DNA by excitation-emission matrix fluorescence coupled with the parallel factor analysis and the alternating normalization weighted error algorithm [26]. Ni et al. reported a fluorescence spectroscopy and chemometrics approach to study the interactions of aspirin and ibuprofen with BSA [27]. To our knowledge, the existing studies just realized the qualitative analysis with emphasis on the variation in the relative concentrations of drug, biomacromolecule and new substance using chemometric methods. There are few studies involving quantitative investigation on dynamic interaction systems, including the amount of free biomacromolecules and free drugs. The request to quantitatively determine free biomacromolecules and free drugs in interaction systems is looming because it contributes to investigating the mechanisms of drug-biomacromolecule interactions and further understanding the bioavailability of drugs in vivo. Varying backgrounds resulting from continually generated new substances during the processes of drug-biomacromolecule interactions often make qualitative or quantitative studies very complicated. An alternative approach is to apply the multi-way calibration method coupled with excitation-emission matrix (EEM) fluorescence, which

can accurately predict concentrations with reasonable resolution of excitation and emission profiles for analyte(s) of interest even in the presence of unknown interferents, that is the "second-order advantage" [28-30]. In a drug-protein interaction system, one can construct a calibration set in a simple buffer solution, where only pure components of interest are included, to predict the concentrations of components in dynamic interaction systems. Then, the obtained quantitative results can be expected to further investigate the binding parameters associated with protein-drug interactions. Furthermore, temperature can have a significant impact on the fluorescence quantum yield and the binding constant, which can't be ignored during the interaction process. Therefore, by introducing a temperature profile as an additional mode, the four-way excitation-emission-temperature-sample data array will be constructed to study the effect of temperature on the protein-drug interaction.

Procaine (PRO), a local anesthetic derived from 4-aminobenzoic acid, shows a short duration of action and adverse side effects, such as cardiac and neurological toxicity [31]. Its short-acting is exerted by the storage in protein and transportation by proteins in blood plasma. To the best of our knowledge, few reports concerning the interaction between PRO and HSA have been found. This paper provides a quantitative determination of the free HSA in the dynamic interaction system with PRO by using second-order calibration method coupled with excitation-emission matrix fluorescence technique, whose schematic illustration is given in Fig. 1. The valuable information concerning spectral and concentration profiles of the free HSA can be extracted from huge amounts of monitoring data from the dynamic HSA-PRO interaction system, and a followed linear regression of the relative HSA concentration values to its real values in calibration set is built for concentration prediction in the binding system. The obtained quantitative results are used for further investigation on the interaction mechanism, including binding constant, binding site number, thermodynamic

parameters and nature of the binding forces. Furthermore, the four-way excitation-emission-temperature-sample data are analyzed to investigate the effect of temperature on the interaction system being studied.

Fig. 1

2. Theory

2.1. Trilinear and quadrilinear component models

If an EEM is assigned to a sample, fluorescence EEMs can be arranged into a three-way array, $\underline{\mathbf{X}}$, of dimensions $I \times J \times K$, where I is the number of excitation wavelengths, J the number of emission wavelengths and K the number of samples. Each element x_{ijk} in the three-way data array $\underline{\mathbf{X}}$ can be expressed by a trilinear component model [32, 33] as follows:

$$x_{ijk} = \sum_{n=1}^{N} a_{in} b_{jn} c_{kn} + e_{ijk}$$
$$(i = 1, 2, ..., I; j = 1, 2, ..., J; k = 1, 2, ..., K.) \qquad (1)$$

Where a_{in}, b_{jn}, and c_{kn} denote the inth, jnth, and knth elements of three underlying profile matrices $\mathbf{A}_{I \times N}$, $\mathbf{B}_{J \times N}$, and $\mathbf{C}_{K \times N}$, respectively, e_{ijk} is the element of three-way residual array $\underline{\mathbf{E}}$ with size of $I \times J \times K$, and N corresponds to the number of components.

The concept of the trilinear component model can be naturally extended to the quadrilinear component model by introducing an additional dimension. In this context, the temperature is associated with variation in fluorescence quantum yield and binding constant, which approximately keeps a linear relationship with fluorescence intensity. Those weak nonlinear factors derived from temperature can be relieved due to the capability of anti-nonlinearity of multi-way data decomposition algorithms. Therefore, fluorescence excitation-emission-temperature data arrays for samples can be arranged into a four-way data array $\underline{\mathbf{X}}_q$, in which each element can be expressed by a

quadrilinear component model [34-36] as follows:

$$x_{ijkl} = \sum_{n=1}^{N} a_{in} b_{jn} c_{kn} d_{ln} + e_{ijkl}$$
$$(i = 1, 2, ..., I; j = 1, 2, ..., J; k = 1, 2, ..., L.) \qquad (2)$$

Where a_{in}, b_{jn}, c_{kn}, and d_{ln} denote the *in*th, *jn*th, *kn*th, and *ln*th elements of four underlying profile matrices $\mathbf{A}_{I\times N}$, $\mathbf{B}_{J\times N}$, $\mathbf{C}_{K\times N}$, and $\mathbf{D}_{L\times N}$, respectively. e_{ijk} is the element of four-way residual array $\underline{\mathbf{E}}_q$ with size of $I\times J\times K\times L$.

3. Experimental

3.1. Reagents and chemicals

All reagents and chemicals used were of analytical grade. Procaine (PRO) (National Institutes for Food and Drug Control, Changsha, China) and human serum albumin (HSA) (Sigma-Aldrich Co. LLC., Shanghai, China) were used without further purification. The chemical structure of procaine was shown in Fig. 2. Ultrapure water was produced by the Milli-Q Gradient A10 system (Millipore, Billerica, USA). Stock solutions of 1.67 mg mL^{-1} PRO and 0.30 mg mL^{-1} HSA were both prepared by dilution in ultrapure water. Stock solutions were stored in a refrigerator at 4°C. The working solutions of PRO and HSA were prepared by the Phosphate Buffered Saline (PBS) buffer, pH 7.4.

Fig. 2

3.2 Fluorescence measurements

In order to quantitative study on interaction between PRO and HSA, three sets of replicated samples were prepared, each including seven calibration samples, six mixed samples and three blank samples. The calibration samples only contained HSA in the concentration range of 4.52×10^{-8}-4.52×10^{-7} mol L^{-1} at seven levels. A series of PRO-HSA mixed solutions were prepared by mixing a constant concentration of HSA solution (4.52×10^{-7} mol L^{-1}) with PRO solution in the concentration range of

3.07×10^{-6}-18.42×10^{-5} mol L^{-1} at six levels. Each set of samples was positioned to run a full reaction for 30 minutes at corresponding temperatures (290 K, 303 K and 310 K). All of fluorometric measurements were carried out on a HITACHI F-7000 fluorescence spectrophotometer (HITACHI, Tokyo, Japan) fitted with a Xenon lamp and interfaced to a personal computer. 1.00 cm quartz cell was used. Fluorescence spectra were recorded in the wavelength ranges of 260-320 nm (excitation) and 300-450 nm (emission). Both excitation and emission slit widths were 5 nm, scan speed was 30000 nm min^{-1}, and detector voltage was 550 V. The spectral data were imported to computer and analyzed in the MATLAB environment.

4. Results and discussion

4.1. Preprocessing the data array

When the samples were measured in the excitation wavelength range (260-320 nm) and the emission wavelength range (300-450 nm), Rayleigh and Raman scatterings appeared in this range. The scatterings, uncorrelated with the analytes, tend to hamper the trilinear structure in the data set. It has to remove this effect. In this paper, an interpolation method was proposed to quickly and effectively handle the scatterings [37]. The interpolation results were shown in Fig. 3 to provide visually sound results, where the scattering regions could be completely removed and the useful fluorescence spectral information still remained well.

Fig. 3

4.2. Characterization of fluorescence spectra

The tryptophan contributes to the dominant intrinsic fluorescence of HSA, and the change of its local environment often leads to variable fluorescence. The intrinsic fluorescence of proteins can therefore provide considerable information about their structure, which is often used to study protein folding

and association reaction. In this work, several different additions of PRO were performed on HSA solution of constant concentration. The fluorescence spectra of HSA were recorded in the absence and presence of PRO as shown in Fig. 4. It was observed that the fluorescence intensity of HSA decreased with increasing concentration of PRO, which implied that the existence of fluorescence quenching was visible and that interaction was found between the HSA and PRO. Moreover, the Fluorescence spectra of HSA-PRO mixtures suggested that heavily overlapping spectra existed between HSA and PRO, which led to quite a bit of trouble selecting the optimal excitation or emission wavelengths for further investigations on this interaction system. Thus, we could turn to the multi-way calibration method in chemometrics to solve the incredibly difficult problem.

Fig. 4

4.3. Quantitation of free HSA using second-order calibration method

4.3.1. Estimation of the number of components

When using trilinear decomposition algorithms to decompose multi-way data arrays into pure spectral profiles of individual constituent, the estimation of the number of underlying factors is of utmost importance. For trilinear decomposition algorithms implemented on multi-way data arrays, some are sensitive to the number of underlying factors, such as parallel factor analysis (PARAFAC) algorithm [33]. In order to ensure the performance of the adopted algorithms and obtain the desired characteristic profiles of the underlying factors and their corresponding relative contributions, it is necessary to estimate the number of underlying factors in multi-way data arrays. In this work, the core consistency diagnostic (CORCONDIA) test [38] was used to determine the number of components. Fig. 5 showed the coreconsistency values as a function of the number of components. The result showed that a three-component model had a core consistency value of 100%, while a

four-component model had a core consistency value of 0%, which meant that three was the appropriate number of components in the interaction system. Among them, two were modeled for HSA and PRO with the remaining one corresponding to the produced unknown interferent. Therefore, the following three-way data array would be decomposed by using three-way decomposition algorithm with $N = 3$.

Fig. 5

4.3.2. Trilinear decomposition

There are many algorithms available for processing multi-way data arrays. The alternating trilinear decomposition (ATLD) algorithm shows an improved performance. The implementation of Moor-Penrose generalized inverse calculation based on truncated single value decomposition makes ATLD insensitive to the overestimated component number and allows for faster convergence. Therefore, the ATLD algorithm was utilized for the decomposition of the obtained three-way data array.

Fig. 6 showed the characteristic profiles obtained from the decomposition of the three-way data array by stacking the excitation-emission fluorescence matrices from different levels of temperature together using the trilinear decomposition algorithm ATLD. The figure indicated that the spectral profiles of HSA were seriously overlapping with those of PRO, resulting in frequent failure to individually determine HSA by traditional spectrophotometry without prior separation. Moreover, there existed a new unknown interferent, whose spectral profiles spread over the spectral range of HSA in both excitation and emission modes. Generally, from the individual fluorescence spectra, it was difficult to deduce the formation of the HSA-PRO complex in the dynamic interaction system due to the significant spectral overlap of constituents. All these made the quantitative analysis of

HSA complicated. However, all the problems have been solved by the second-order calibration method. Three-way data analysis allows concentration and spectral profiles of the sample components to be extracted even in the presence of unexpected constituents. As was shown in the Fig. 6, concentrations and spectral profiles were achieved well using the trilinear decomposition algorithm ATLD. As comparison, the dotted lines denoted the corresponding actual spectra of HSA. It could be observed that the resolved excitation and emission spectral profiles of HSA were nearly the same as the actual ones, which indicated that the obtained results were accurate and reliable. The squared correlation coefficients between the decomposed and measured spectra in excitation and emission modes were 0.9951 and 0.9973 for HSA, respectively. In the Figure 6C, it was obvious that the concentration of HSA declined linearly with the increasing concentration of PRO, which implied an interaction between HSA and PRO. Moreover, the concentration of the unknown constituent showed a linear upward trend. The point was further clarified that a new fluorescent substance was produced in the dynamic interaction system being studied.

Fig. 6

For the quantitative investigation on the dynamic interaction system, the free HSA and PRO concentrations should be both obtained. In the present work, the concentration of free PRO could be approximately equal to the total concentration of added PRO as a consequence of the added PRO concentration far more than ten times of HSA concentration in the experimental design. Therefore, the determination of free HSA became a critical issue. Following the trilinear decomposition, the classical linear regression of decomposed relative concentration profile corresponding to HSA against its real concentration was built (in Fig. 7), and further used to predict the actual concentration of HSA in the dynamic interaction system at corresponding temperatures. The squared correlation

coefficients were 0.9993, 0.9978 and 0.9993 at 290 K, 303 K, and 310 K in calibration set, respectively, which were regarded as sound linear fits at different temperatures. The obtained results were listed in Table 1. The results showed that the second-order calibration method could achieve the quantitative analysis of the free HSA in dynamic interaction systems with drug molecules, even in the presence of unknown interferents. It could be concluded that the second-order calibration method characterizing the "second-order advantage" was an effective and reliable technique to monitor the concentrations of components of interest in complex and dynamic interaction systems.

Fig. 7

Table 1

4.4. The influence of temperature by four-way data analysis

In order to study the effect of temperature on the dynamic interaction system between HSA and PRO, an extra dimension, namely temperature mode, was introduced. A four-way data array could be therefore obtained by joining third-order data for a set of mixture samples into a four-dimensional mathematical object. The dimension of the four-way data array was 30×75×3×5, where 30 corresponded to the excitation mode, 75 to the emission mode, 3 to the temperature mode and 5 to the sample mode. For purpose of the feasibility of various multi-way decomposition algorithms for multi-way data arrays, the four-way alternating weighted residue constraint quadrilinear decomposition (AWRCQLD) [39] with the component number N = 3 was applied for the decomposition of the obtained four-way data array.

The result of the quadrilinear decomposition was given in Fig. 8, where the obtained pure excitation, emission, temperature, and concentration profiles of constituents in the PRO-HSA dynamic interaction system were plotted correspondingly. The resolved excitation and emission

spectra of HSA from the quadrilinear decomposition were very consistent with those measured from individual standards (dash-dot lines), which were also in high accordance with the resolved results from trilinear decomposition. The correlation coefficients between the decomposed and measured spectra in excitation and emission modes were 0.9996 and 0.9993 for HSA respectively. Furthermore, the profiles of an unknown and dynamic intereferent corresponding to the HSA-PRO complex were extracted as expected. It illustrated that the quadrilinear decomposition can extract profiles from huge amounts of monitoring data in the dynamic interaction system.

Fig. 8

The temperature will produce a significant impact on the fluorescence quantum yield and the binding constant, which can't be ignored in investigation on interaction systems. In the resolved temperature mode, the relative intensities of HSA and PRO decreased along with the temperature, while the relative intensity of unknown product increased. It could be explained that the temperature had more effects on the fluorescence quantum yield than on the binding constant. Moreover, a similar tendency between HSA and PRO, as reactants, led to the high collinearity in the temperature mode. The collinearity caused a frequent failure in trilinear decomposition of three-way data analysis. However, the quadrilinear decomposition could settle the problem of high collinearity, which was an additional advantage. In the fourth mode, the concentrations of the analytes, including HSA, PRO and the HSA-PRO complex, showed the same variation trend with those obtained from the trilinear decomposition. Considering the high consistency between the trilinear decomposition and quardrilinear decomposition about the obtained profiles, a conclusion could be made that the multi-way calibration method could provide a promising and convenient alternative to study on a interaction system, qualitatively and quantitatively.

4.5. Binding constant and binding sites

The binding of HSA with PRO to form complex in the ground state was further understood on the basis of quantitative information obtained from the multi-way calibration analysis. On the assumption that there are n substantive binding sites for drug (Q) on protein (B), the binding reaction can be shown as follows [40, 41]:

$$nQ + B \rightleftharpoons Q_n B \qquad (3)$$

The binding constant K can be calculated as:

$$K = \frac{[Q_n B]}{[Q]^n [B]} \qquad (4)$$

Where $[Q]$ and $[B]$ are the drug molecular and protein concentration, respectively, $[Q_n B]$ is the concentration of drug-HSA complex, K is the binding constant and n corresponds to the number of binding sites.

$$[Q_n B] = [B_0] - [B] \qquad (5)$$

$$K = \frac{[B_0] - [B]}{[Q]^n [B]} \qquad (6)$$

$$\log\left(\frac{[B_0] - [B]}{[B]}\right) = \log K + n \log[Q] \qquad (7)$$

where $[B_0]$ is assigned to the initial HSA concentration. In the present work, based on $[B_0]$, $[Q]$ and the obtained $[B]$ from multi-way data analysis, linear plots of $\log\left(\frac{[B_0] - [B]}{[B]}\right)$ versus $\log[Q]$ were obtained (Fig. 9). Values of $\log K$ and n were derived from a weighted least-square fit to the points in Fig. 9. The results were summarized in Table 2. It showed that the binding constants for the HSA-PRO system decreased with the increasing temperature. Furthermore, the significant large values of K at different temperatures, which ranged from 0.82×10^6 to 2.04×10^6 L mol^{-1}, showed a

relatively high affinity for the binding of PRO to HSA. The values of n approximately equal to 1 indicated the existence of just a single binding site in HSA for PRO.

Fig. 9

Table 2

4.6. Thermodynamic parameters and nature of the binding forces

The interaction forces between small molecules and biological macromolecules mainly include hydrogen bonds, van der Waals force, hydrophobic and electrostatic interactions, and so on [40]. The information associated with thermodynamic parameters, including free energy (ΔG), enthalpy (ΔH), and entropy (ΔS) of interaction, are required to interpret the binding mode. ΔG reflects the possibility of reaction, while ΔH and ΔS are mainly responsible for judging the nature of the binding forces. In the field of thermodynamics, a judgment is accepted that $\Delta H > 0$ and $\Delta S > 0$ imply hydrophobic forces, $\Delta H < 0$ and $\Delta S < 0$ van der Waals forces and hydrogen bonds, and $\Delta H < 0$ and $\Delta S > 0$ electrostatic forces [42]. The binding parameters of HAS-PRO complex were evaluated via the Van't Hoff equation, where the linear relation between $\ln K$ and $1/T$ holds. And then, ΔH and ΔS would be obtained from the plot of $\ln K$ versus $1/T$.

$$\ln K = -\Delta H / RT + \Delta S / R \qquad (8)$$

ΔH can be regarded as a constant when the temperature does not vary significantly. Further, the free energy changes (ΔG) at different temperatures can be calculated by the following equation:

$$\Delta G = \Delta H - T\Delta S = -RT \ln K \qquad (9)$$

Here, R is the gas constant and K is the binding constant at the corresponding experimental temperature. According to the obtained binding constants K of HSA-PRO interaction system at three temperatures from the multi-way data analysis, the thermodynamic functions involved in the binding

process could be obtained, as showed in Fig. 10. It could be seen that the negative ΔH and negative ΔS values indicated the major role of van der Waals forces and hydrogen bonds in the formation of the HSA-PRO complex. The crystal structure analyses showed that the principle regions of ligand binding sites in albumin were located in hydrophobic cavities in subdomains ⅡA and ⅢA [43]. The sole tryptophan residue, located in subdomains ⅡA in HSA, played an important role in the binding of drugs to subdomain ⅡA because of the formation of hydrogen bond between drugs and tryptophan. According to the structure of procaine, the strong polar amino group, a substitute group on the benzene ring, is easy to form hydrogen bond with tryptophan. Therefore, the hydrogen bond is most likely to promote the formation of the procaine-HSA complex, which is in accordance with the deduction from the values of calculated thermodynamic parameters. The formation of hydrogen bond meant that the higher the temperature, the weaker the bond between HSA and PRO, which was also verified by the decreasing values of K with increase in temperature in Table 2. Meanwhile, the negative values of ΔG showed a characterization of spontaneity for the binding reaction between HSA and PRO.

Fig. 10

5. Conclusion

An effective and sensitive method was proposed for quantitative determination of the free human serum albumin (HSA) in the dynamic interaction system with procaine (PRO) even in the presence of uncalibrated and continually produced interferent. The determination of free HSA concentration in complex and dynamic systems was realized with the aid of the second-order calibration method characterizing “second-order advantage”, and then the results were used to further calculate the binding parameters. Furthermore, the four-way data analysis was used to qualitatively and visually

show effect of temperature on the dynamic HSA-PRO interaction system. Beyond the specific application in HSA-PRO dynamic interaction system, the proposed multi-way calibration method could be expected to provide significant insight into quantitative analysis in dynamic systems, such as hydrolysis kinetics, enzymatic reaction, drug metabolism, etc.

Acknowledgements

The authors gratefully acknowledge the National Natural Science Foundation of China (No. 21175041), the National Basic Research Program (No. 2012CB910602), and the Foundation for Innovative Research Groups of NSFC (No. 21221003) for financial supports.

Reference

1. W. E. Müller and U. Wollert, Pharmacology, 1979, 19, 59-67.
2. J. Tang, F. Luan and X. Chen, Biorg. Med. Chem., 2006, 14, 3210-3217.
3. D. C. Carter and J. X. Ho, Adv. Protein *Chem.*, 1994, 45, 153-203.
4. Y. Z. Zhang, B. Zhou, Y. X. Liu, C. X. Zhou, X. L. Ding and Y. Liu, *J. Fluoresc.*, 2008, 18, 109-118.
5. G. Sudlow, D. Birkett and D. Wade, *Mol. Pharmacol.*, 1975, 11, 824-832.
6. G. Sudlow, D. Birkett and D. Wade, *Mol. Pharmacol.*, 1976, 12, 1052-1061.
7. L. Trynda-Lemiesz and H. Kozlowski, *Biorg. Med. Chem.*, 1996, 4, 1709-1713.
8. J. Kang, Y. Liu, M. X. Xie, S. Li, M. Jiang and Y. D. Wang, *BBA-Gen. Subjects*, 2004, 1674, 205-214.
9. Y. L. Wei, J. Q. Li, C. Dong, S. M. Shuang, D. S. Liu and C. W. Huie, *Talanta*, 2006, 70, 377-382.
10. G. Zhang, N. Zhao, X. Hu and J. Tian, *Spectrochim. Acta A*, 2010, 76, 410-417.

11. X. R. Pan, P. F. Qin, R. T. Liu and J. Wang, *J. Agric. Food Chem.*, 2011, 59, 6650-6656.

12. H. Sanei, A. Asoodeh, S. Hamedakbari-Tusi and J. Chamani, *J. Solution Chem.*, 2011, 40, 1905-1931.

13. Y. Ni, S. Su and S. Kokot, *Anal. Chim. Acta*, 2006, 580, 206-215.

14. A. Muñoz de la Peña, A. Espinosa Mansilla, D. González Gómez, A. C. Olivieri and H. C. Goicoechea, *Anal. Chem.*, 2003, 75, 2640-2646.

15. H. B. Wang, Y. J. Zhang, X. Xiao, S. H. Yu and W. Q. Liu, *Anal. Methods*, 2011, 3, 688-695.

16. F. Cañada-Cañada, A. Espinosa-Mansilla, A. M. de la Peña, A. J. Girón and D. González-Gómez, *Food Chem.*, 2009, 113, 1260-1265.

17. X. D. Zhong, D. S. Fu, P. P. Wu, Q. Liu, G. C. Lin, S. H. Cao and Y. Q. Li, *Anal. Methods*, 2014, 6, 7260-7267.

18. R. M. Maggio, P. C. Damiani and A. C. Olivieri, *Anal. Chim. Acta*, 2010, 677, 97-107.

19. A. Baum, A. S. Meyer, J. L. Garcia, M. Egebo, P. W. Hansen and J. D. Mikkelsen, *Anal. Chim. Acta*, 2013, 778, 1-8.

20. A. Baum, P. W. Hansen, A. S. Meyer and J. D. Mikkelsen, *Anal. Chim. Acta*, 2013, 790, 14-23.

21. Y. Ni, G. Liu and S. Kokot, *Talanta*, 2008, 76, 513-521.

22. R. Liu, Z. Cheng, T. Li and X. Jiang, *J. Lumin.*, 2015, 157, 398-410.

23. M. B. Gholivand, A. R. Jalalvand, H. C. Goicoechea, R. Gargallo and T. Skov, *Talanta*, 2015, 132, 354-365.

24. Q. Zhang, Y. Ni and S. Kokot, *J. Agric. Food. Chem.*, 2013, 61, 7730-7738.

25. X. Zhu, Y. Lu, J. Wang and Q. Xu, *Analytical Methods*, 2013, 5, 6037-6044.

26. H. Y. Zou, H. L. Wu, Y. Zhang, S. F. Li, J. F. Nie, H. Y. Fu and R. Q. Yu, *J. Fluoresc.*, 2009, 19,

955-966.

27. Y. Ni, R. Zhu and S. Kokot, *Analyst*, 2011, 136, 4794-4801.

28. E. Sanchez and B. R. Kowalski, *J. Chemom.*, 1988, 2, 265-280.

29. H. L. Wu, J. F. Nie, Y. J. Yu and R. Q. Yu, *Anal. Chim. Acta*, 2009, 650, 131-142.

30. G. M. Escandar, H. C. Goicoechea, A. Muñoz de la Peña and A. C. Olivieri, *Anal. Chim. Acta*, 2014, 806, 8-26.

31. C. Lazdunski and D. Baty, *Eur. J. Biochem.*, 1979, 96, 49-57.

32. J. D. Carroll and J. J. Chang, *Psychometrika*, 1970, 35, 283-319.

33. R. A. Harshman, *UCLA Working Papers in Phonetics*, 1970, 16, 1-84.

34. A. K. Smilde and D. A. Doornbos, *J. Chemom.*, 1991, 5, 345-360.

35. G. M. Escandar, A. C. Olivieri, N. K. M. Faber, H. C. Goicoechea, A. Muñoz de la Peña and R. J. Poppi, *TrAC, Trends Anal. Chem.*, 2007, 26, 752-765.

36. C. Kang, H. L. Wu, Y. J. Yu, Y. J. Liu, S. R. Zhang, X. H. Zhang and R. Q. Yu, *Anal. Chim. Acta*, 2013, 758, 45-57.

37. M. Bahram, R. Bro, C. Stedmon and A. Afkhami, *J. Chemom.*, 2006, 20, 99-105.

38. R. Bro and H. A. Kiers, *J. Chemom.*, 2003, 17, 274-286.

39. H. Y. Fu, H. L. Wu, Y. J. Yu, L. L. Yu, S. R. Zhang, J. F. Nie, S. F. Li and R. Q. Yu, *J. Chemom.*, 2011, 25, 408-429.

40. Y. J. Hu, Y. Liu, J. B. Wang, X. H. Xiao and S. S. Qu, *J. Pharm. Biomed. Anal.*, 2004, 36, 915-919.

41. A. Belatik, S. Hotchandani, J. Bariyanga and H. A. Tajmir-Riahi, *Eur. J. Med. Chem.*, 2012, 48, 114-123.

42. P. D. Ross and S. Subramanian, *Biochemistry (Mosc).* 1981, 20, 3096-3102.

43. O. K. A. Z. and O. I. K. A. S., *J. Am. Chem. Soc.*, 2008, 130, 10793-10801.

Legends to Figures and Tables

Fig. 1 Schematic illustration of quantitative determination of the free HSA in a dynamic interaction system.

Fig. 2 The chemical structure of procaine.

Fig. 3 Landscapes of the mixture sample 5 before handling the scatterings (A) and after handling the scatterings (B).

Fig. 4 Fluorescence landscapes of HSA in the presence of PRO: (A) mixture sample 01; (B) mixture sample 02; (C) mixture sample 03; (D) mixture sample 04; (E) mixture sample 05; (F) mixture sample 06.

Fig. 5 Result of the core consistency.

Fig. 6 The spectral profiles obtained from the decomposition of the three-way data array using the alternating trilinear decomposition (ATLD) algorithm: (A) excitation mode; (B) emission mode; (C) concentration mode.

Fig. 7 Results of regression in the three-way calibration method at different temperatures: (A) 290K; (B) 303K; (C) 310K.

Fig. 8 The spectral profiles obtained from the decomposition of the four-way data array using the alternating weighted residue constraint quadrilinear decomposition (AWRCQLD) algorithm: (A) excitation mode; (B) emission mode; (C) temperature mode; (D) concentration mode.

Fig. 9 Plots of log $[(B_0 - B)/B]$ versus log [Q] at different temperatures.

Fig. 10 Plots of ln$K$ versus -1/T at different temperatures.

Table 1 Results of quantitative analysis in mixture samples obtained by three-way calibration method.

Table 2 Binding constants, numbers of binding sites and free energy changes in different temperatures.

Graphical and textual abstract

An effective and sensitive method is provided for quantitative investigation on the dynamic interaction of human serum albumin with procaine using multi-way calibration method coupled with three-dimensional fluorescence spectroscopy. The free human serum albumin in dynamic interaction system is quantified, and their interaction mechanism is also studied. Furthermore, the four-way excitation-emission-temperature-sample data are analyzed to investigate the effect of temperature on the interaction system studied.

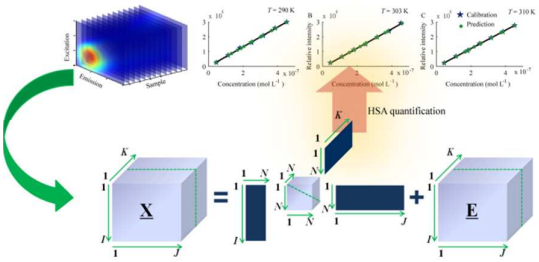

Table 1 Results of quantitative analysis in mixture samples obtained by three-way calibration method.

sample	**Added** (10^{-7} mol L^{-1})	(10^{-6} mol L^{-1})	**Predicted** (10^{-7} mol L^{-1})		
	HSA	**PRO**	**HSA** (290K)	**HSA** (303K)	**HSA** (310K)
#01	4.52	3.07	3.66	3.62	3.76
#02	4.52	6.14	3.05	3.07	3.18
#03	4.52	9.21	2.55	2.58	2.63
#04	4.52	12.28	2.13	2.18	2.22
#05	4.52	15.35	1.67	1.91	1.93
#06	4.52	18.42	1.37	1.58	1.63

Table 2 Binding constants, numbers of binding sites and free energy changes in different temperatures.

Temperature /K	**N**	**log*K***	***K*** /10^6 L mol^{-1}	**△*G*** /kJ mol^{-1}
290	1.20	6.31	2.04	-34.89
303	1.20	5.93	0.85	-34.83
310	1.20	5.91	0.82	-34.80

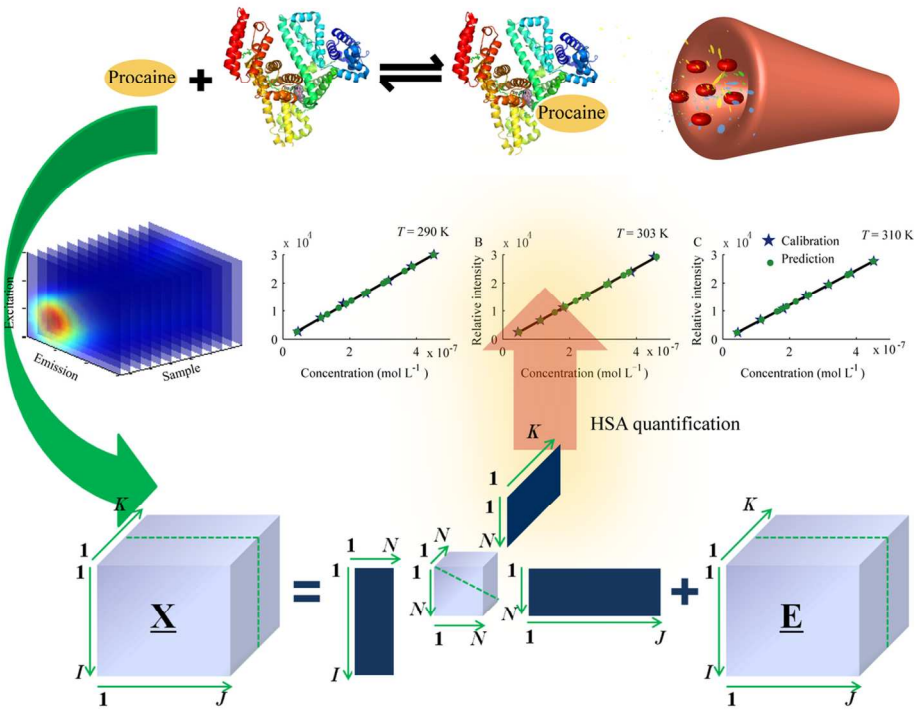

Fig. 1 Schematic illustration of quantitative determination of the free HSA in a dynamic iteraction system.
116x86mm (300 x 300 DPI)

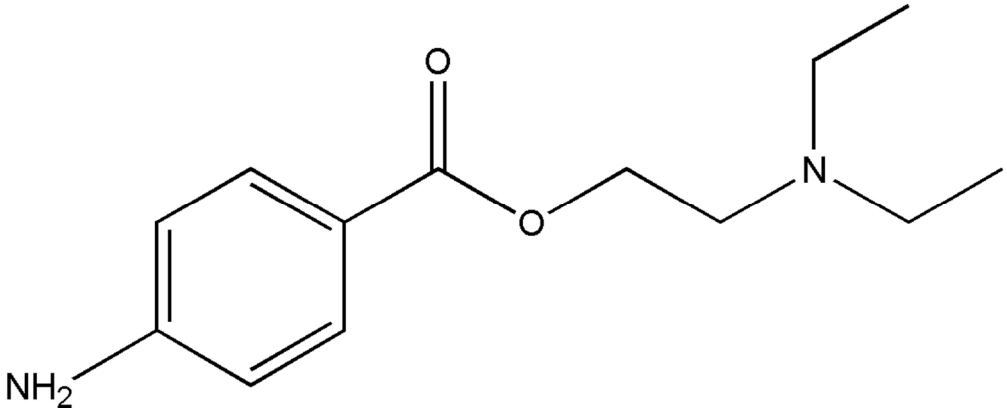

Fig. 2 The chemical structure of procaine.
97x39mm (300 x 300 DPI)

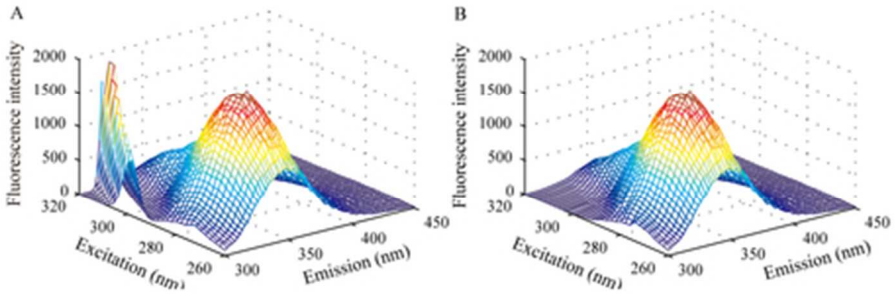

Fig. 3 Landscapes of the mixture sample 5 before handling the scatterings (A) and after handling the scatterings (B).
43x13mm (300 x 300 DPI)

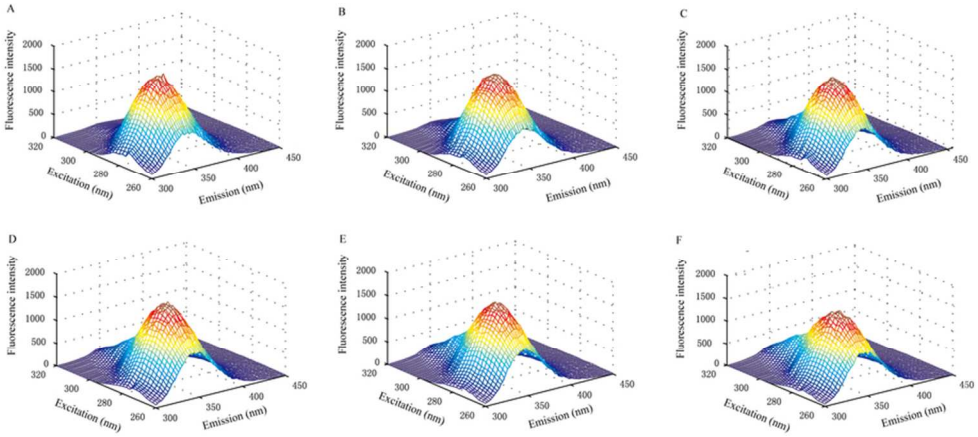

Fig. 4 Fluorescence landscapes of HSA in the presence of PRO: (A) mixture sample 01; (B) mixture sample 02; (C) mixture sample 03; (D) mixture sample 04; (E) mixture sample 05; (F) mixture sample 06.
79x34mm (300 x 300 DPI)

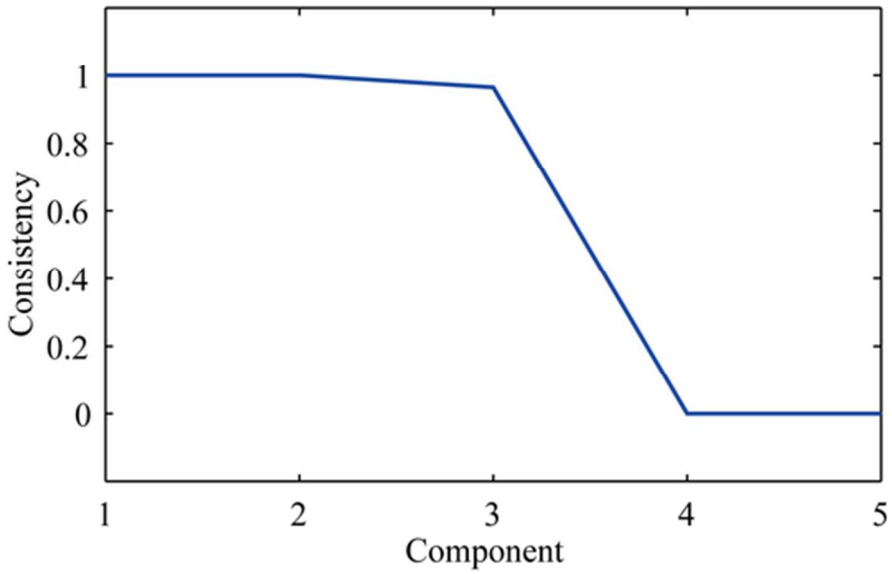

Fig. 5 Result of the core consistency.
51x31mm (300 x 300 DPI)

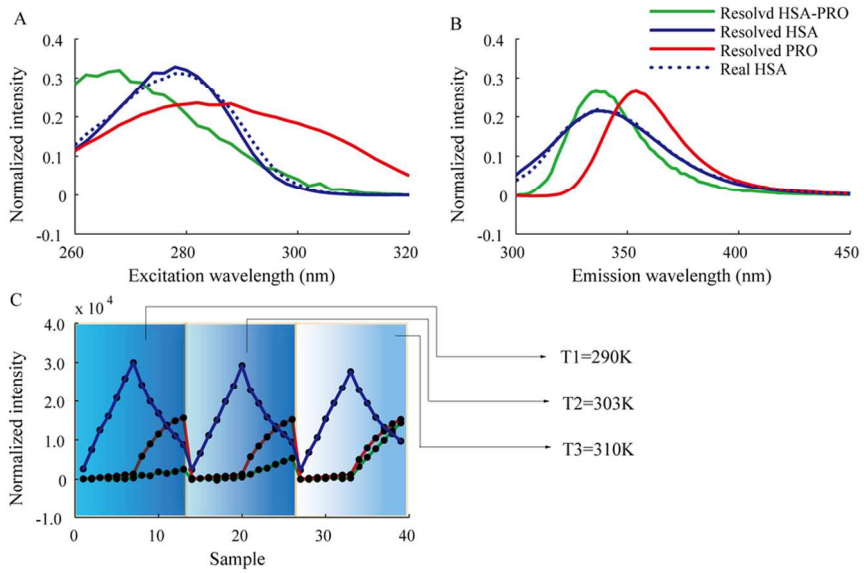

Fig. 6 The spectral profiles obtained from the decomposition of the three-way data array using the alternating trilinear decomposition (ATLD) algorithm: (A) excitation mode; (B) emission mode; (C) concentration mode.
102x61mm (300 x 300 DPI)

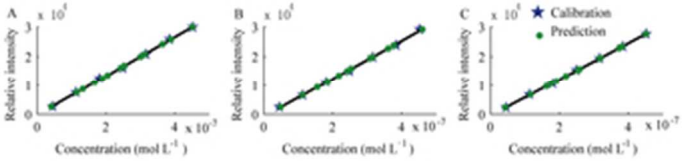

Fig. 7 Results of regression in the three-way calibration at different temperatures: (A) 290K; (B) 303K; (C) 310K.
34x6mm (300 x 300 DPI)

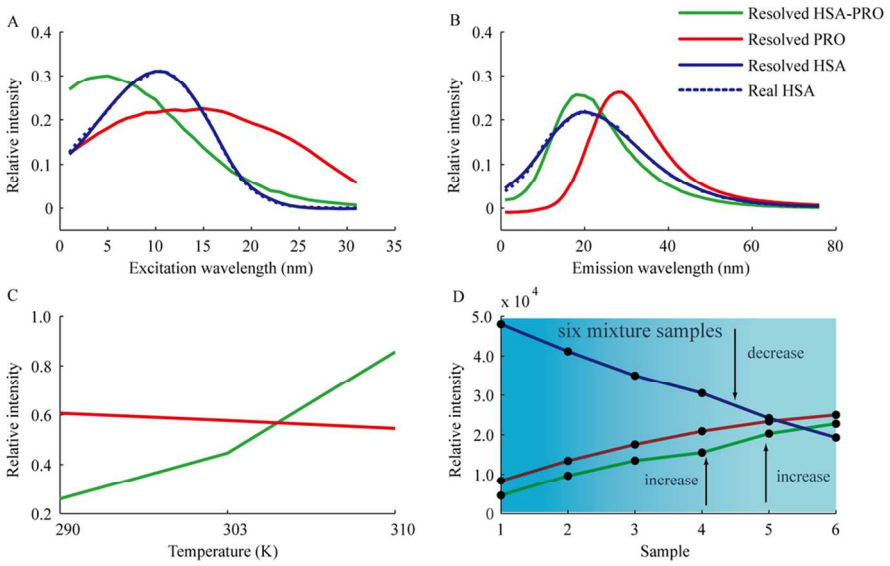

Fig. 8 The spectral profiles obtained from the decomposition of the four-way data array using the alternating weighted residue constraint quadrilinear decomposition (AWRCQLD) algorithm: (A) excitation mode; (B) emission mode; (C) temperature mode; (D) concentration mode.
102x61mm (300 x 300 DPI)

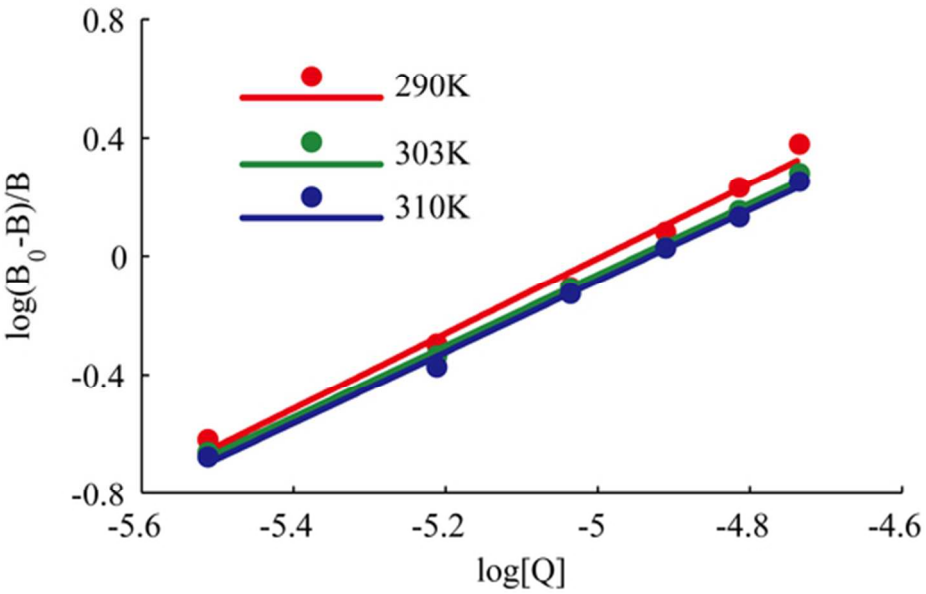

Fig. 9 Plots of log [(B0− B)/B] versus log [Q] at different temperatures.
51x31mm (300 x 300 DPI)

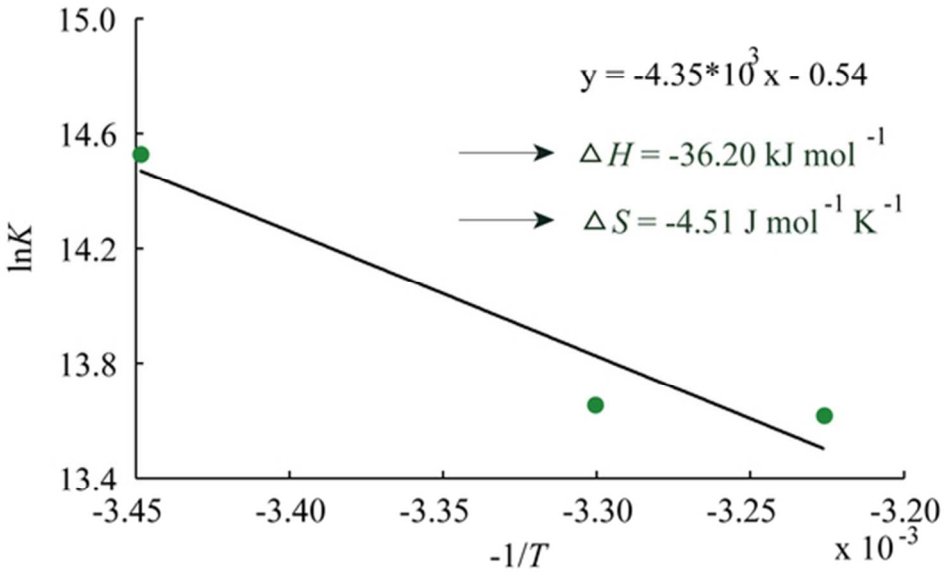

Fig. 10 Plots of lnK versus -1/T at different temperatures.
51x31mm (300 x 300 DPI)